IEEE Access
Multidisciplinary | Rapid Review | Open Access Journal

Received August 31, 2020, accepted September 22, 2020, date of publication October 12, 2020, date of current version October 21, 2020.

Digital Object Identifier 10.1109/ACCESS.2020.3030103

Novel Monitoring System for Low-Voltage DC Distribution Network Using Deep-Learning-Based Disaggregation

JIN-WOOK LEE[1], KEON-JUN PARK[1], (Member, IEEE), JINTAE CHO[2], JU-YONG KIM[2], AND SUNG-YONG SON[1], (Member, IEEE)

[1]Department of Electrical Engineering, Gachon University, Seongnam 13120, South Korea
[2]Smart Power Distribution Laboratory, Korea Electric Power Corporation Research Institute (KEPRI), Daejeon 34056, South Korea

Corresponding author: Sung-Yong Son (xtra@gachon.ac.kr)

This work was supported in part by Korea Electric Power Corporation (KEPCO) under Grant R15DA12, in part by the Korea Institute of Energy Technology Evaluation and Planning (KETEP), in part by the Ministry of Trade, Industry, and Energy (MOTIE) of the Republic of Korea under Grant 20191210301650, and in part by the Gachon University under Grant GCU-2019-0801.

ABSTRACT The deployment rate of distributed energy resources (DER) based on renewable energy has recently been increasing worldwide. Direct current (DC) power distribution has been proposed as an efficient approach for operating digital loads and DC-based renewable energy. DC distribution systems with DERs, however, are not commonly used in the real world. From the viewpoint of distribution system operators, it is important to identify the operation status of DERs for effective grid operation. In this article, a novel monitoring methodology for low-voltage DC (LVDC) distribution systems with DERs is proposed based on frequency-domain analyses. A deep-learning technology is applied to model the frequency characteristics of individual DERs. A case study considering two approaches was conducted using a photovoltaic generator, wind turbine, diesel generator, and energy-storage system installed in an LVDC testbed operated by KEPCO in Gochang, Jeolla-do, Korea. In the first approach, monitoring is performed with sensors installed near individual DERs. In the second approach, monitoring is performed with a single sensor in the distribution line, and the signal is disaggregated to identify the status of the individual DERs. The results show that the proposed methodology tracks the status of DERs with an accuracy of 98% and 95%, respectively, demonstrating the validity of the proposed methodologies.

INDEX TERMS LVDC, distribution, deep learning, FFT, monitoring, disaggregation, tracking.

I. INTRODUCTION

Recently, the deployment rate of digital loads and distributed energy resources (DERs) based on renewable energy has been increasing worldwide [1]. Renewable energy sources (RESs) such as photovoltaic systems (PVs) and battery electric vehicles (EVs) are DC-based energy sources that can be integrated into the grid in the form of DERs [2]. Because RESs have high output uncertainty, an energy storage system (ESS) is necessary to compensate for this uncertainty [3], [4]. The prevailing power system infrastructure is based on alternating current (AC), while the leading environmentally friendly energy sources such as PVs, EVs, and ESSs, produce DC power [5].

Currently, power system infrastructure that is capable of incorporating ESSs and RESs usually converts the DC power produced by these energy sources to AC. This adds complexity and reduces the efficiency of the power system because of the need for a power converter [6], [7]. Furthermore, an increasing number of DC-consuming devices such as computers, televisions, and monitors are being integrated into buildings [8]. The power supplied to these devices must be converted again from AC back to DC, adding further losses and complexity to the power system [8], [9]. Thus, DC architectures for electric power-distribution systems are being increasingly explored, with the goal of serving most modern loads that require DC power more efficiently [10]. Furthermore, technologies related to low-voltage DC (LVDC) distribution networks are being actively researched to improve the distribution efficiency, power quality, and reliability [11]–[13].

The associate editor coordinating the review of this manuscript and approving it for publication was Fabio Massaro.

Monitoring is one of the critical issues in LVDC networks because of the lack of operational experience. If DERs such as PV, WT, and ESS are integrated into the LVDC distribution network, unexpected situations may arise depending on the operations of the DERs. To solve these operational problems, the following methods can monitor DERs:

First, real-time monitoring of all individual DERs would be preferable. However, this is not possible because of the high cost and excessive effort associated with installation. Second, indirect monitoring can be conducted through the voltage and current of an arbitrary bus in the distribution system to which many DERs are connected. Here, disaggregation technology extracts features of different signal sources from a mixed signal [14], [15]. Third, the two abovementioned methods in the LVDC distribution network have limited monitoring parameters to track the operation status of the individual DERs. For clearer tracking and disaggregating operating status, DER-specific modeling is required through frequency values generated during operation that can verify unique characteristics. Finally, the long-lasting monitoring in the LVDC distribution network results in a large amount of data accumulation. A deep-learning-based system is required to efficiently utilize these data for monitoring engines. The monitoring signals generated by DERs are highly complex because they are related to the amount of generation, which changes continuously. Deep learning is an appropriate technology to solve this type of problem [16], [17]. Generation-source tracking and disaggregation technology using deep learning have greatly improved in terms of robustness and generalization ability compared with traditional tracking methods [18]–[21]. In this work, two approaches are used for DER output tracking in an LVDC distribution system. One is to install sensors immediately next to each DER and assume that smart meters and/or protection devices will perform real-time monitoring. The other is to install a single sensor in the distribution line (DL). The data obtained from the single sensor consist of complex signals, which are the operation signals of DERs and other power-distribution equipment. The monitored data contained in this complex signal are disaggregated through deep learning to identify the statuses of individual DERs.

In this article, a novel LVDC monitoring system using deep-learning-based disaggregation is proposed. Disaggregation is performed on the frequency signal of the voltage, and fast Fourier transform (FFT) analyses were performed at a sampling rate of 100 kHz. The frequency characteristics of each DER are learned through deep learning. The operation status of each DER for monitoring was modeled. As a result, the validity of the estimation under complex system situations is verified.

The remainder of this article is organized as follows. An overview of LVDC distribution network monitoring is presented in Section II. In Section III, deep-learning models for LVDC distribution network monitoring are described. The case study results are presented and discussed in Section IV. Finally, Section V concludes the paper.

II. APPROACHES FOR LVDC DISTRIBUTION MONITORING

LVDC and low-voltage AC (LVAC) distribution networks exhibit several commonalities and differences with respect to monitoring. The topology, components, and general monitoring parameters are mostly the same in both distribution systems. However, because of the differences in electrical characteristics, some of the parameters are more significant in the AC system than in the DC system, and the reverse is true for some parameters. This section describes the characteristics of the LVDC distribution, which should be considered for monitoring, the configuration of the LVDC distribution topology, and the methodology for monitoring in the frequency domain.

A. DC DISTRIBUTION CHARACTERISTICS

The characteristics of the DC power-distribution system are different from those of the existing AC power-distribution systems [22].

First, both AC and DC have different electrical properties. AC has a physical characteristic called a sine wave, while DC has a straight wave. Second, the parameters that can be analyzed for monitoring are limited by the electrical characteristics [23]. In the case of AC, voltage, current, active power, reactive power, and harmonics are usually considered. However, in the case of DC, the power factor, reactive power, and frequency do not exist; therefore, the elements that can be monitored are limited. Third, the number of PCSs connected to the distribution system is lower in the DC distribution than in the AC distribution.

Therefore, the noise detection result of the PCS is clearer and more accurate. In the LVDC distribution system, because the signal can be analyzed based on the switching frequency of the DER's PCS in the frequency domain, an approach to track and disaggregate the characteristic frequency signal of the DER in the LVDC distribution is proposed in this article.

B. APPROACHFOR LVDC MONITORING

Nonintrusive load monitoring (NILM) is one of the algorithms for monitoring the operation of household loads at the customer end of the AC distribution system [24]. It is an algorithm that disaggregates the signals of several appliances in a home from the power signal integrated at the distribution board [25]. As a result, NILM helps determine the operation status and electricity consumption of each home appliance [26]. This information enables economical home-energy management.

In this article, low-voltage DC monitoring (LDCM), a monitoring methodology for an LVDC distribution system, is proposed to observe the DER operation status. LDCM applies an NILM-based monitoring algorithm. The environment of LDCM is changed from the (existing) consumer stage to the distribution stage, and the scale of targets is changed from appliances to DERs. Table 1 shows the similarities and differences between the AC NILM and LDCM.

TABLE 1. NILM vs LDCM.

	NILM	*LDCM*
Num. of Points	Single	Single/Multi
Location	Panel board	DER/ DL
Backbone	AC	DC
Parameters	V, I, W, Var, VA, Harmonics	V, I, W, Freq. spectrum

In general, NILM involves a single monitoring point on a power panel board. The monitoring parameters of NILM are usually voltage, current, real and reactive powers, and harmonics. However, LDCM can be performed with single or multiple monitoring points at the DERs or along the DL. The monitoring parameters of the LDCM are the voltage, current, real power, and frequency spectrums. Therefore, the number of monitoring parameters of the LDCM is less than that of the conventional NILM because of the DC characteristics.

C. COMPONENTS OF THE LVDC DISTRIBUTION SYSTEM

For monitoring, a proper understanding of LVDC distribution-system components is necessary. The LVDC distribution network generally consists of distributed generators (DG), inverters, DC–DC converters, storage systems, and loads. Fig. 1 shows the configuration of an LVDC distribution system. The power equipment and devices that constitute the LVDC distribution systems may have different voltage levels, current capacities, and operation settings. Power conversion systems (PCSs) are adopted to integrate these devices and equipment into the grid by changing their voltage outputs to control the power flow amount and direction. It is common to use pulse-width modulation (PWM) control technology to obtain the required voltage outputs. PWM is performed based on the so-called switching frequency, which causes high-frequency noises [27].

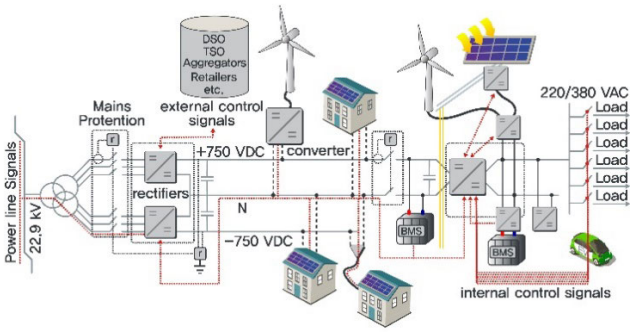

FIGURE 1. Configuration of LVDC distribution system.

D. MONITORING IN FREQUENCY DOMAIN

The fundamental frequency of AC is generally set at 50 or 60 Hz, depending on the grid environment. Harmonics in the form of a distorted sinusoid are commonly used to describe high-frequency noises in AC systems. However, there is no fundamental frequency in the DC. The fundamental frequency in DC is generally considered to be 0 Hz. However, a DC system has high-frequency noise signals in the DC distribution line, which are mostly caused by PCSs. Individual PCSs have characteristic switching frequencies and generate corresponding noise patterns. When each equipment is connected to the DC grid via a PCS, we can estimate the operation status of each connected equipment by observing the DC DL noise [26].

III. MODELING FOR LVDC DISTRIBUTION NETWORK MONITORING

A. LVDC MONITORING SYSTEM ARCHITECTURE

When customer-owned DERs are integrated into an LVDC distribution system, the operational complexity of the system increases. Grid operators prefer to know the exact statuses of individual DERs for their operation. In order to know the status such as voltage, current, or power of individual DERs, it is common to install a data-acquisition device for each DER. However, this is usually not possible when many DERs are involved in terms of the cost and practicality of installation.

The voltage signal in a DL contains composite noise signals from all power devices and DERs connected to the grid. If we can separate the characteristic signals of individual DERs appropriately, we can estimate the operation status of the DERs.

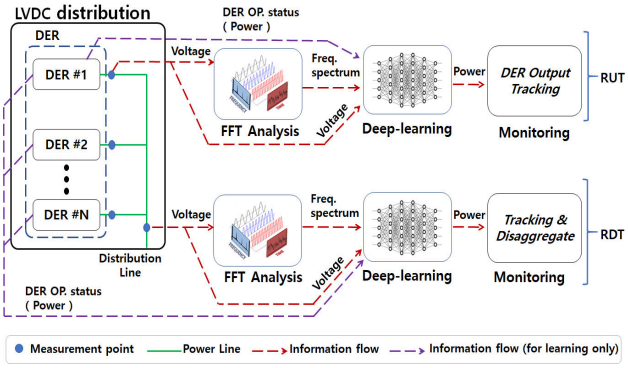

FIGURE 2. Schematic of LVDC Distribution Network Monitoring System.

In this study, two deep-learning-based approaches are used and compared for DER monitoring in an LVDC network: resource unit tracking (RUT) and resource disaggregation and tracking (RDT). Fig. 2 shows the concepts of RUT and RDT. In the RUT approach, the sensors are installed for individual devices, and a deep-learning model is trained separately with the frequency spectrum of the voltage and status data of each DER output side. In the RDT approach, a single sensor is installed in the DL, and the deep-learning model is trained with the frequency spectrum of the DL voltage and the status data of all DERs. In both cases, the measured voltage is analyzed to build the characteristic frequency through FFT analysis. This characteristic frequency is used to develop a

deep neural network (DNN) for monitoring. Then, the trained deep learning model can track the DER output through the voltage.

B. DEEP-LEARNING MODELING

An artificial neural network (ANN) is a network modeled by simulating the neurons in the human brain, and is described through the connections between neurons in the form of a nonlinear system. The most representative ANN is the multi-layer perceptron (MLP). The MLP consists of an input layer that receives a signal, a hidden layer that carries and expresses a signal, and an output layer that combines the results [28], [29].

Deep learning is a type of ANN that overcomes the limitations of conventional networks by solving the problem of a vanishing gradient and overfitting with the innovation of computing power [30], [31]. A deep neural network (DNN) is an ANN with multiple layers in the hidden layer. A DNN has as many neurons in the input layer as the number of input vectors to represent a nonlinear system, and the number of outputs to be obtained is the number of neurons in the output layer. The number of layers and number of neurons in the hidden layer are determined by the designer, depending on the problem to be solved. A DNN can be expressed by (1) to (3):

$$\mathbf{a}^0 = \mathbf{x} \tag{1}$$

$$\mathbf{a}^{l+1} = f^{l+1}\left(\mathbf{w}^{l+1}\mathbf{a}^l + \mathbf{b}^{l+1}\right), \quad for\ l = 0, 1, \ldots, L-1 \tag{2}$$

$$\mathbf{y} = \mathbf{a}^L \tag{3}$$

where $\mathbf{x}$ is the input vector, and$\mathbf{a}$ is the output vector of neurons in the layer. $\mathbf{w}$ and $\mathbf{b}$ are the connection weights and bias vectors, respectively. $f(\cdot)$ is the activation function, and L is the number of layers in the network. $\mathbf{y}$ is the output vector of the model. The activation function in the hidden layer and output layer can be used by (4) and (5), namely, a leaky rectified linear unit (leaky-Relu) [32] and linear activation function, respectively.

$$f(x) = \max(0.01x, x) = \begin{cases} x & x \geq 0 \\ 0.01x & x < 0 \end{cases} \tag{4}$$

$$f(x) = x. \tag{5}$$

A DNN requires a learning algorithm to learn from the data. The learning algorithm uses a backpropagation algorithm, which is a supervised learning method that reduces the error between a target value and the output value of the model. The backpropagation algorithm calculates the error and propagates the error back to each layer, in the direction along which the defined loss function is minimized, to learn the connection weights of neurons [33]. There are several learning algorithms, including Adagrad [34], RMSProp [35], and Adam [36]. Fundamentally, the loss function is given by (6).

$$E(\theta) = \frac{1}{2}\sum_{k=1}^{K}\left(y_k - \hat{y}_k\right)^2 \tag{6}$$

where E is the objective function, θ is the learning parameter, y_k is the k-th target output, $\hat{y}_k$ is the k-th model output, and k is the number of outputs. Learning of parameters is carried out using (7) and (8)

$$\boldsymbol{\theta}_{t+1} = \boldsymbol{\theta}_t + \Delta\boldsymbol{\theta}_t \tag{7}$$

$$\Delta\boldsymbol{\theta}_t = -\eta\frac{\partial E}{\partial \boldsymbol{\theta}_t} \tag{8}$$

where η is a positive learning rate.

In this study, deep learning was applied to track the operating state of individual DERs in the LVDC distribution system and to disaggregate the operating state of individual DERs from the multiple operating states of the DERs. To this end, the deep learning model is designed using the characteristic frequencies of DERs as the input variables and the powers of the DERs as the output variables.

C. LVDC MONITORING PROCESS

In order to analyze and monitor the data collected from the LVDC distribution system, a DNN-based monitoring process was designed, as shown in Fig. 3. The process supports both the RUT and RDT approaches.

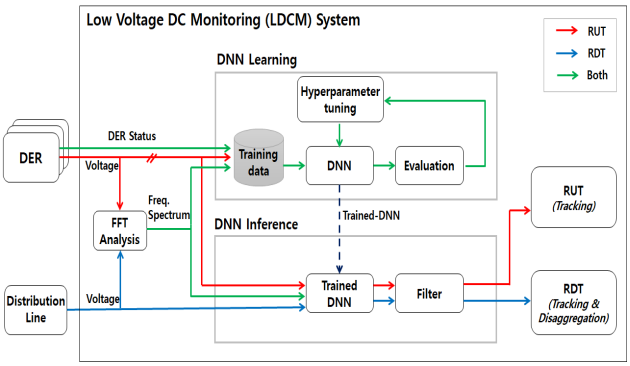

FIGURE 3. Schematic diagram of LVDC monitoring process.

In the RUT, data such as voltage and power are collected when each of the DERs is operated in the LVDC distribution network, and the DNN is modeled by training the frequency signals of voltage through FFT analysis. The monitoring locations of the RUT are the outputs of the DERs. The RUT tracks and monitors the operation status and output variation of each DER.

In the RDT, the signal of each DER is disaggregated from an integrated signal, such as voltage or power, by monitoring the DL of the grid when multiple DERs are integrated in the LVDC distribution network, and the operation status and each output are estimated. Specifically, overlapping characteristic signals of DERs in the frequency domain are disaggregated to each DER's power characteristic, and the power of each DER is estimated through the amplitude size in the frequency domain.

The DNN model, which is the core of the LVDC monitoring process, is trained from the monitoring data. The DNN model was verified and evaluated using the validation data. Based on the results of the evaluation, the hyperparameters

that are set before the learning process begin are tuned. Then, the DNN model is retrained depending on the results. As a result, the trained model uses test data to output the model prediction results and monitor the status of the DER. A pre-processing filter is used to remove the noise and ripple in the raw output.

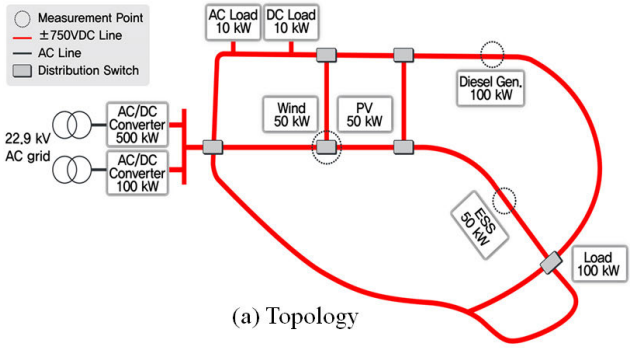

(a) Topology

(b) Aerial photographic map

FIGURE 4. Configuration of KEPCO LVDC testbed in Gochang, South Korea.

IV. CASE STUDY

A. GOCHANG LVDC DISTRIBUTION TEST OF KEPCO

The LVDC distribution testbed of the Korea Electric Power Corporation (KEPCO) Power Test Center in Gochang, Jeollado, Korea was used in this work. The testbed consisted of a grid topology, as shown in Fig. 4. The main voltage of the LVDC testbed was bipolar ±750 VDC. It contained DERs such as PVs, WTs, battery ESSs, and diesel generators as well as AC and DC loads. All DERs and loads were connected to the grid through power electronic devices. The main AC/DC converters interconnected the LVDC distribution system to a 22.9 kV medium-voltage AC grid. In our experiments, a diesel generator (50 kW), PV (50 kW), WT (50 kW), ESS (50 kW), and load (100 kW) were used, as shown in Table 2. Voltage changes were measured using a DEWE-2600 at a sampling rate of 100 kHz.

B. RESOURCE CHARACTERISTIC FREQUENCY

The main switching frequencies of the PCS for the diesel generator, PV, WT, and ESS were 7.2 kHz, 10 kHz, 5 kHz, and 11 kHz, respectively, as described in Table 2.

TABLE 2. Specifications of distributed energy resources.

	Capacity [kW]	PCS Switching Frequency [kHz]
Diesel generator	100	7.2
PV	50	10
WT	50	5
ESS	50	11

Fig. 5 shows the time series of the frequency spectrum according to the output changes of the DERs. The characteristic frequency patterns mainly appear in each PCS switching frequency band and its multiples. The diesel generator's characteristic frequencies appear at 7.2 kHz and 14 kHz. The characteristic frequencies of the PV are at 10 kHz and its multiples. In the case of PV, the signal is weaker than that of the other PCS of DERs. Therefore, it is difficult to identify the status of the DERs using the distribution noise.

Moreover, relatively strong noise is observed when the output is idle. The WT pattern shows relatively high amplitude characteristics at 5 kHz and 20–30 kHz, when compared to that of the other DERs. In particular, around the 30 kHz band, a wide range of characteristic frequencies are detected. For the ESS, the characteristic frequencies are detected at 11 kHz, 30 kHz, and 50 kHz. In particular, the frequency characteristics are relatively high at 11 kHz, which is the PCS switching frequency band. The frequency spectrum strength tends to increase when the DER output increases, which can be used to estimate the output of the DERs.

C. RESULTS OF LDCM

Experiments were conducted for DER output tracking and disaggregation from the real site, which was in the testbed of the KEPCO PT center. The training data comprised 20 h in total, and the test set comprised 2 h. The datasets used in the single DER tracking, RUT, and RDT are shown in Tables 3 and 4, respectively.

TABLE 3. Datasets for single DER test.

	Train data	Valid. data	Test data
Diesel Gen.	102,342	20,468	81,873
PV	161,718	32,343	129,373
WT	206,558	41,311	165,246
ESS	370,312	74,062	296,249

In single DER, RUT, and RDT, the training and validation data sets were configured in a ratio of 8:2, respectively. In addition, the test dataset was separately configured in different time zones that were not measured in the training and validation data. Three test sets were used to evaluate the performance of the models. The first was a test set for a single

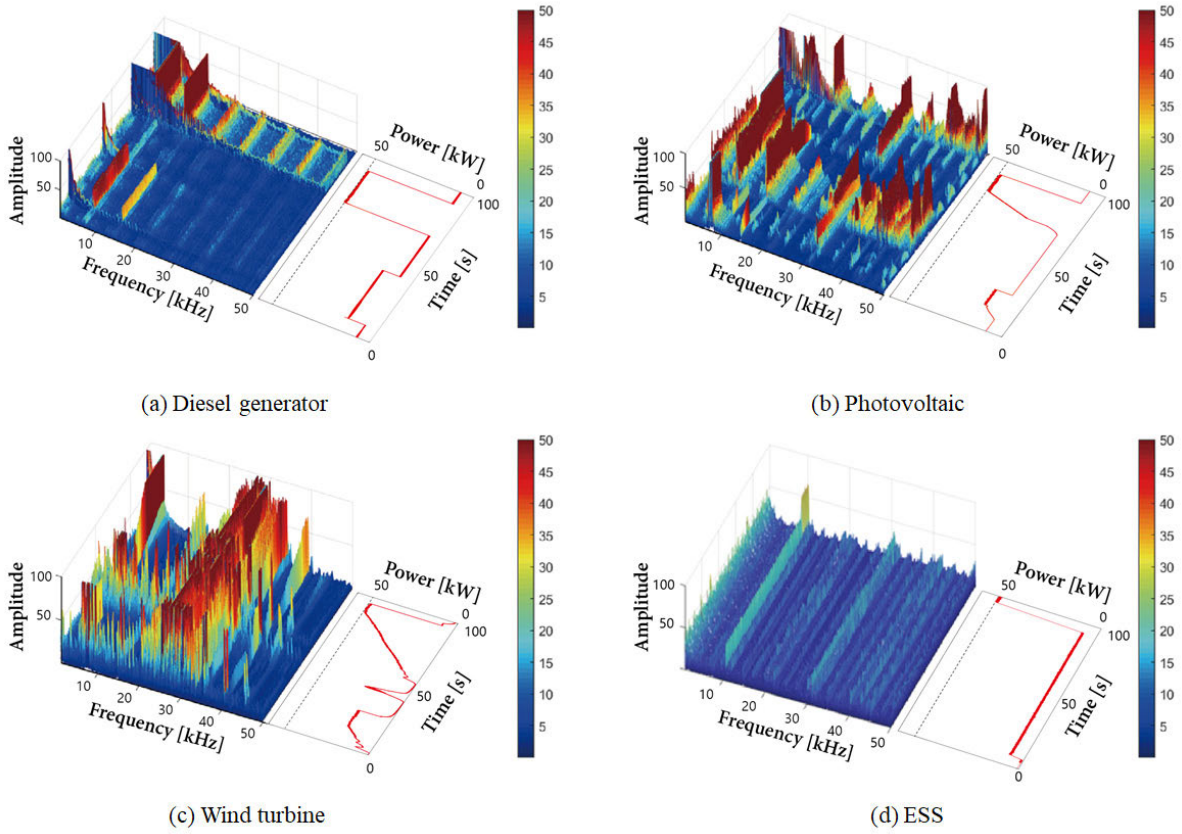

FIGURE 5. Time series of frequency spectrum of DER.

TABLE 4. Datasets for RUT and RDT.

	Train data	Valid. data	Test data
RUT, RDT	570,056	114,011	103,349

DER test, the second one was for RUT, and the last one was for RDT.

All DNN models used in this study have the same architecture. In the case of a single DER test and RDT, the input to the network is a 257-dimensional vector consisting of one voltage and the amplitudes of 256 frequency bands. In RUT, the input to the network is a 1,028 (257 × 4)-dimensional vector consisting of each DER's voltage and the amplitudes of 256 frequency bands. For all models, the output consists of DER powers. The hidden layer consists of 512-32-16 networks. After the hidden layer, the output for the RUT is a one-dimensional vector and that for the RDT is a four-dimensional vector. The activation function of each layer is a leaky rectified linear unit function, and the optimizer is an Adam optimizer. The Savizky–Golay filter was used as the post-processing filter. For deep learning, 10 repeated experiments were performed for each parameter change. The test performance index for evaluation is based on the mean squared error (MSE) and mean absolute error (MAE).

1) SINGLE DER

Before verifying the RUT and RDT, output tracking was performed using the data of each DER operating condition to verify whether the learning performance based on the frequency characteristics was valid.

Fig. 6 shows the output tracking results of the DER (diesel generator, PV, WT, and ESS) powers. In Fig. 6, the blue line represents the real target output and the red line depicts the result of the model output, both of which are compared. Fig. 6(a) – (d) show a single DER test result of a diesel generator, PV, WT, and ESS, respectively.

From the results, it can be observed that the output of each DER is tracked with a high performance of over 98%. Here, 100% performance means complete detection over the entire estimation time. The test results of this learning model are shown in terms of the MSE and MAE, in Table 5.

2) RUT

This section analyzes the performance results of the RUT designed in the previous section. Fig. 7 shows the disaggregated results, which are the powers of the individual DERs. Each color depicts each DER's measurement data and model output.

Fig. 8(a) – (d) show the power tracking results of the individual DERs. The black line depicts the real target output,

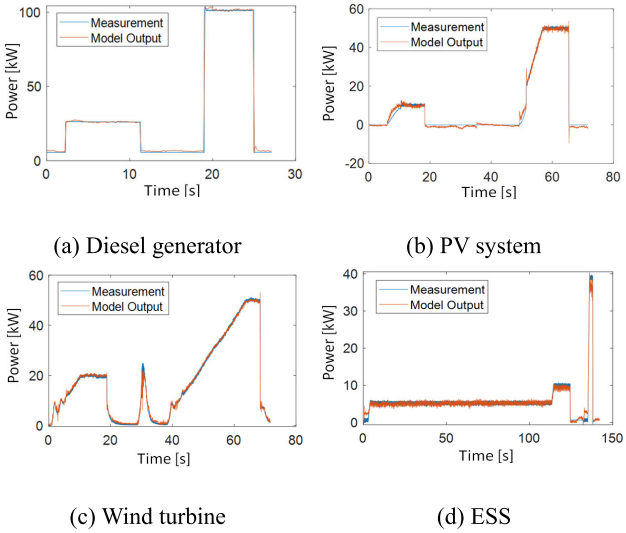

(a) Diesel generator (b) PV system

(c) Wind turbine (d) ESS

FIGURE 6. Sample of DER output tracking results.

TABLE 5. Test results of single DER test.

	MSE	MAE
Diesel	0.034	0.094
PV	0.084	0.102
WT	0.028	0.062
ESS	0.104	0.168

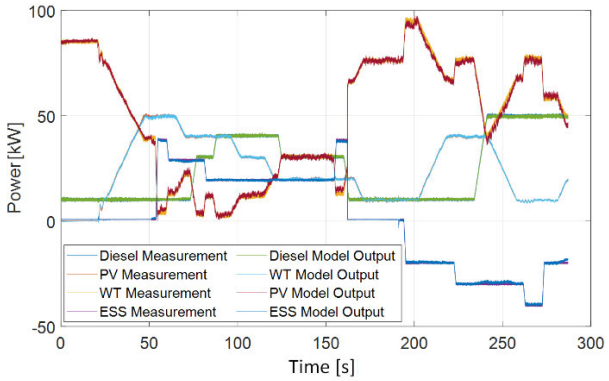

FIGURE 7. Results of RUT for all DERs.

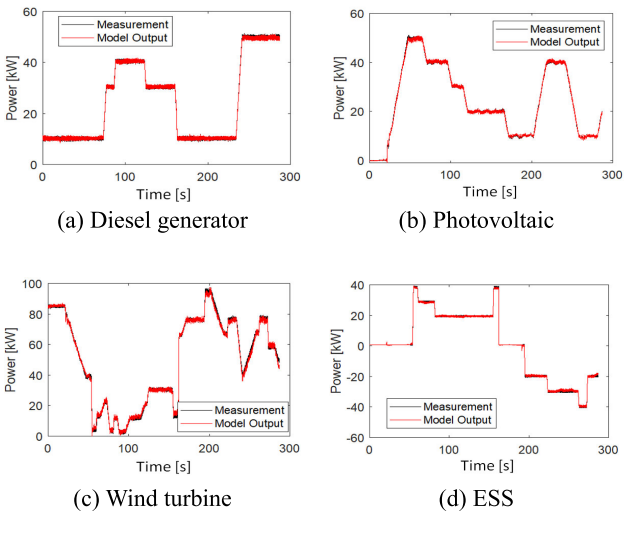

(a) Diesel generator (b) Photovoltaic

(c) Wind turbine (d) ESS

FIGURE 8. Results of RUT for each DER.

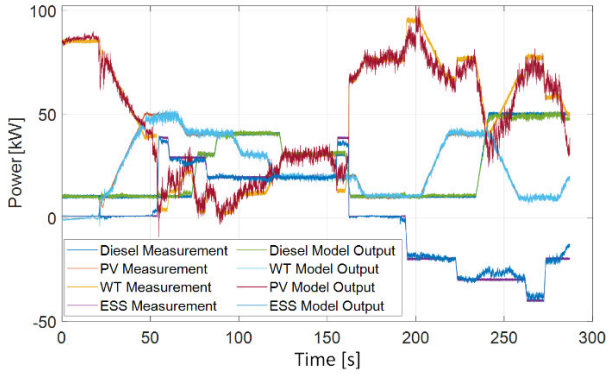

FIGURE 9. Results of RDT for all DERs.

TABLE 6. Test results of estimation performance.

	RUT		*RDT*		*Δ RDT-RUT*	
	MSE	MAE	MSE	MAE	MSE	MAE
Diesel	0.044	0.091	0.058	0.196	0.014	0.105
PV	0.091	0.117	0.178	0.204	0.087	0.087
WT	0.034	0.074	0.066	0.123	0.032	0.049
ESS	0.134	0.197	0.225	0.375	0.091	0.178
Model	0.076	0.120	0.132	0.225	0.056	0.105

and the red line represents the model output. By performing RUT, the output of each DER can be tracked with a high performance of over 95.8%. The numerical test results of this model are shown in terms of the MSE and MAE in Table 6.

3) RDT

This section analyzes the experimental performance results of the RDT designed in the previous section. Fig. 9 shows the disaggregated results, which are the powers of the individual DERs. Each color depicts each DER's measurement data and model output.

Fig. 10(a) – (d) show the power tracking results of the individual DERs. The black line depicts the real target output, and the red line represents the model output. By performing RDT, the output of each DER can be disaggregated with a high performance of over 91.5%. The result shows reasonable performance when compared with the NILM performance for houses [37]. The numerical test results of this model are shown in terms of the MSE and MAE in Table 6.

Table 6. shows the performance of each model for RUT and RDT and the performance difference between the two models. Here, Δ RDT-RUT represents the performance difference between the two models.

In the case of the RUT, which is a model that individually tracks the operation status signals of each DER, the tracking performance of each DER is 0.036 for diesel, 0.091 for PV,

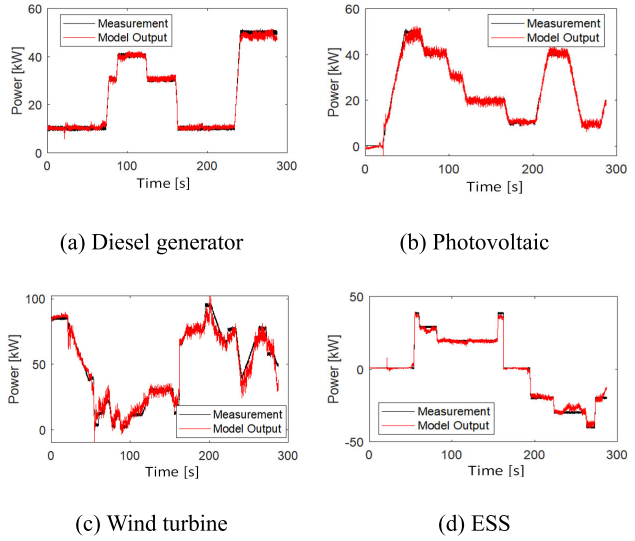

FIGURE 10. Results of RDT for each DER.

0.118 for WT, and 0.134 for ESS. The average performance for the four DERs was 0.095. Diesel has the best tracking performance, followed by PV, WT, and ESS. In the case of the ESS, the tracking performance of the operation state is the lowest when in the charged state. RUT is possible when the DER operation status is monitored individually.

RDT is a model that disaggregates the operation status of each DER through DL signals, and the tracking performance through DER disaggregation based on MSE is 0.058, 0.127, 0.191, and 0.225, respectively, for diesel, PV, WT, and ESS. The average model performance for all the DERs is 0.15. The operation status tracking performance of DER through RDT is shown in the order of diesel, PV, WT, and ESS. The performance of RDT was found to be slightly lower than that of the RUT. In particular, the switching characteristic frequency of WT is mixed with various frequencies that are difficult to distinguish, unlike other DERs. Because the switching characteristic frequency band of the WT overlaps with that of the PV, the tracking performance of RDT is lower than that of RUT. Similar to the result of RUT, in the case of ESS, ripple occurs more frequently when charging.

When comparing RUT and RDT, the average performance difference for the four DERs is 0.056, and the performance of the RDT is rather low. The difference in performance of DERs is 0.022 for diesel, 0.036 for PV, 0.073 for WT, and 0.091 for ESS. Diesel and PV show similar performance differences, and WT and ESS show somewhat higher performance differences. In addition, performance indicators based on MAE generally show results similar to those based on MSE.

Through this experiment, each DER has a switching characteristic frequency, so it can be confirmed that it is possible to monitor the operating status in the LVDC distribution network. However, to monitor the operation status of all DERs, a measurement device must be installed in all DERs. From a physical and economic point of view, there may be limitations in monitoring by installing measuring devices on all DERs. However, it has been confirmed that although the performance is somewhat lower than that of individual monitoring, it is possible to monitor by substituting the disaggregation of superimposed signals by measuring the electrical signals of DL.

D. DISCUSSIONS

1) SENSITIVITY ANALYSIS OF NOISE

One of the factors influencing the performance of the proposed RDT model is the noise level of the voltage. To verify the performance of the proposed model, a sensitivity analysis with respect to the noise level of voltage was performed. The noise level applied was from 0 to 20% of the voltage of the test data.

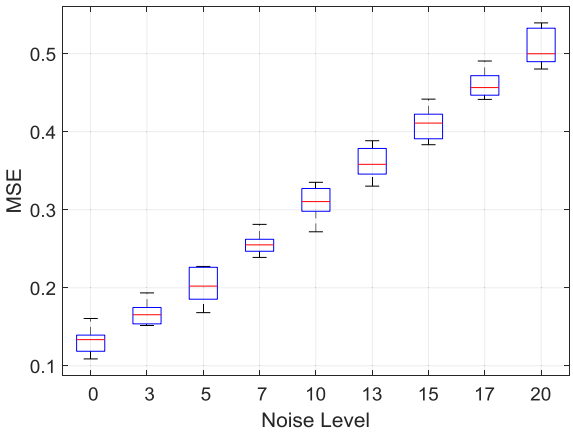

FIGURE 11. Sensitivity of noise level for RDT.

Fig. 11 shows the sensitivity to the RDT model performance according to the noise level of the test data. As the white noise increases up to 20%, the model performance error of the RDT tends to increase by an average of 40% for each level, and the deviation in each step is 0.03-0.05, showing a linear sensitivity characteristic.

2) SYSTEM SCALABILITY

As the scale of the system increases, it would be increasingly difficult to identify all the devices with a single point measurement. However, the signals generated by a generation source attenuate as the distance increases. Therefore, the problem scale does not increase significantly because signals arising in far-away places become background noise. The individual size of each zone would have a limited number of sources with sufficient strength, even though the signals of the generators are not completely separated. Multi-point learning can also improve the performance when the target zone size increases.

3) GENERATION UNCERTAINTIES

In this work, the learning would have limitations because supervised learning was applied. However, if the learning is performed with appropriate variations, then the effect of uncertainty can be considered. In the real world, the learning

would be conducted over a long period of time, including uncertainty effects in nature.

V. CONCLUSION

In this article, a deep-learning-based monitoring methodology that monitors the status of individual DER-connected grids by tracking the DER directly and disaggregating the voltage of the DL in the LVDC distribution network in a KEPCO PT center is proposed. The findings and contributions of this study are as follows.

- ➢ Applying the proposed LDCM methodology. LDCM was designed through an extension of NILM considering the characteristics of the LVDC distribution network.
- ➢ FFT analysis for characterization of the PCS switching frequency of DER. The characteristic frequencies were derived through FFT analysis of the four DERs, and it was confirmed that the characteristic frequencies have a high correlation with the PCS switching frequency of each DER.
- ➢ Proposed deep-learning-based RUT and RDT model verification. The RUT and RDT have been designed by supervised learning along with the characteristic frequency of DER, and the proposed methodologies have been validated by demonstrating high performance.
- ➢ Sensitivity analysis of the RDT model. As the noise level of the distribution network increases up to 20%, the proposed RDT model increases linearly. This means that the proposed RDT model has robust characteristics for noise levels up to 20% with respect to the original signal.

Further research will include a methodology for harmonizing and monitoring complex signals generated in various zones of the LVDC distribution network. This will involve monitoring and analyzing abnormal conditions or contingency events such as malfunctions, breakdowns, and deterioration.

REFERENCES

[1] P. Wang, L. Goel, X. Liu, and F. H. Choo, "Harmonizing AC and DC: A hybrid AC/DC future grid solution," *IEEE Power Energy Mag.*, vol. 11, no. 3, pp. 76–83, May 2013.
[2] J. Feng, B. Zeng, D. Zhao, G. Wu, Z. Liu, and J. Zhang, "Evaluating demand response impacts on capacity credit of renewable distributed generation in smart distribution systems," *IEEE Access*, vol. 6, pp. 14307–14317, 2018.
[3] A. Kwasinski and A. Kwasinski, "Operational aspects and power architecture design for a microgrid to increase the use of renewable energy in wireless communication networks," in *Proc. Int. Power Electron. Conf. (IPEC-Hiroshima ECCE ASIA)*, Hiroshima, Japan, May 2014, pp. 2649–2655.
[4] A. Kwasinski and A. Kwasinski, "Role of energy storage in a microgrid for increased use of photovoltaic systems in wireless communication networks," in *Proc. IEEE 36th Int. Telecommun. Energy Conf. (INTELEC)*, Vancouver, BC, Canada, Sep. 2014, pp. 1–8.
[5] M. Starke, L. M. Tolbert, and B. Ozpineci, "AC vs. DC distribution: A loss comparison," in *Proc. IEEE/PES Transmiss. Distribution Conf. Exposit.*, Chicago, IL, USA, Apr. 2008, pp. 1–7.
[6] M. Szpek, B. J. Sonnenberg, and S. M. Lisy, "400 VDC distribution architectures for central offices and data centers," in *Proc. IEEE 36th Int. Telecommun. Energy Conf. (INTELEC)*, Vancouver, BC, Canada, Sep. 2014, pp. 1–6.
[7] M. Noritake, K. Yuasa, T. Takeda, H. Hoshi, and K. Hirose, "Demonstrative research on DC microgrids for office buildings," in *Proc. IEEE 36th Int. Telecommun. Energy Conf. (INTELEC)*, Vancouver, BC, Canada, Sep. 2014, pp. 1–5.
[8] H. Kakigano, Y. Miura, and T. Ise, "Low-voltage bipolar-type DC microgrid for super high quality distribution," *IEEE Trans. Power Electron.*, vol. 25, no. 12, pp. 3066–3075, Dec. 2010.
[9] M. Salato, A. Zolj, D. J. Becker, and B. J. Sonnenberg, "Power system architectures for 380V DC distribution in telecom datacenters," in *Proc. Intelec*, Scottsdale, AZ, USA, Sep. 2012, pp. 1–7.
[10] Electric Power Research Institute (EPRI). *DC Power Production, Delivery and Utilization*. Accessed: Oct. 2020. [Online]. Available: http://directpowertech.com/docs/EPRI_DCpower_WhitePaper_June2006FINAL.pdf
[11] J.-W. Shin, H. Shin, G.-S. Seo, J.-I. Ha, and B.-H. Cho, "Low-common mode voltage H-bridge converter with additional switch legs," *IEEE Trans. Power Electron.*, vol. 28, no. 4, pp. 1773–1782, Apr. 2013.
[12] D. Dong, I. Cvetkovic, D. Boroyevich, W. Zhang, R. Wang, and P. Mattavelli, "Grid-interface bidirectional converter for residential DC distribution systems—Part one: High-density two-stage topology," *IEEE Trans. Power Electron.*, vol. 28, no. 4, pp. 1655–1666, Apr. 2013.
[13] D. Dong, F. Luo, X. Zhang, D. Boroyevich, and P. Mattavelli, "Grid-interface bidirectional converter for residential DC distribution systems—Part 2: AC and DC interface design with passive components minimization," *IEEE Trans. Power Electron.*, vol. 28, no. 4, pp. 1667–1679, Apr. 2013.
[14] X. He, Q. Ai, R. C. Qiu, W. Huang, L. Piao, and H. Liu, "A big data architecture design for smart grids based on random matrix theory," *IEEE Trans. Smart Grid*, vol. 8, no. 2, pp. 674–686, Mar. 2017.
[15] X. He, L. Chu, R. C. Qiu, Q. Ai, and Z. Ling, "A novel data-driven situation awareness approach for future grids—Using large random matrices for big data modeling," *IEEE Access*, vol. 6, pp. 13855–13865, 2018.
[16] G. Wu, W. Lu, G. Gao, C. Zhao, and J. Liu, "Regional deep learning model for visual tracking," *Neurocomputing*, vol. 175, pp. 310–323, Jan. 2016.
[17] H. Grabner, C. Leistner, and H. Bischof, "Semi-supervised on-line boosting for robust tracking," in *Proc. Eur. Conf. Comput. Vis. (ECCV)*, 2008, pp. 234–247.
[18] Z. Hu, H. Chen, and G. Li, "Deep ensemble object tracking based on temporal and spatial networks," *IEEE Access*, vol. 8, pp. 7490–7505, 2020.
[19] J. Heikkila and O. Silven, "A four-step camera calibration procedure with implicit image correction," in *Proc. IEEE Comput. Soc. Conf. Comput. Vis. Pattern Recognit.*, San Juan, PR, USA, 2008, pp. 1106–1112.
[20] S. W. Park, J. Cho, J. Kim, and S. Y. Son, "Design for low voltage DC distribution network testbed," *Int. J. Eng. Technol.*, vol. 7, no. 3, pp. 264–267, Aug. 2018.
[21] Y. C. Y. Cho, J. K. J. Kim, J. C. J. Cho, and J. K. J. Kim, "Design and construction of LVDC distribution site," in *Proc. CIRED Workshop*, Helsinki, U.K., 2016, pp. 1–4.
[22] M. Zeifman and K. Roth, "Nonintrusive appliance load monitoring: Review and outlook," *IEEE Trans. Consum. Electron.*, vol. 57, no. 1, pp. 76–84, Feb. 2011.
[23] S. S. Hosseini, K. Agbossou, S. Kelouwani, and A. Cardenas, "Non-intrusive load monitoring through home energy management systems: A comprehensive review," *Renew. Sustain. Energy Rev.*, vol. 79, pp. 1266–1274, Nov. 2017.
[24] J. Lee, S.-Y. Son, E. Oh, T. H. Kim, and J. Y. Kim, "Load monitoring effects and characteristics of DC home," in *Proc. IEEE Int. Conf. Consum. Electron. (ICCE)*, Las Vegas, NV, USA, Jan. 2018, pp. 1–2.
[25] E. J. Kim, C.-H. Cho, W. Kim, C.-H. Lee, and J. Laskar, "Spurious noise reduction by modulating switching frequency in DC-to-DC converter for RF power amplifier," in *Proc. IEEE Radio Freq. Integr. Circuits Symp.*, Anaheim, CA, USA, 2010, pp. 43–46.
[26] C. M. Bishop, *Neural Network for Pattern Recognition*. Oxford, U.K.: Oxford Univ. Press, 1995, pp. 332–380.
[27] M. Negnevitsky, *Artificial Intelligence: A Guide to Intelligent Systems*, 3rd ed. Reading, MA, USA: Addison-Wesley, 2011.
[28] G. E. Hinton, S. Osindero, and Y.-W. Teh, "A fast learning algorithm for deep belief nets," *Neural Comput.*, vol. 18, no. 7, pp. 1527–1554, Jul. 2006.
[29] Y. LeCun, Y. Bengio, and G. Hinton, "Deep learning," *Nature*, vol. 521, pp. 436–444, May 2015.
[30] A. L. Maas, A. Y. Hannun, and A. Y. Ng, "Rectifier nonlinearities improve neural network acoustic models," in *Proc. 30th Int. Conf. Mach. Learn.*, vol. 28. Atlanta, GA, USA: W and CP, Jun. 2013, p. 3.

[31] D. E. Rumelhart, G. E. Hinton, and R. J. Williams, "Learning representations by back-propagating errors," *Nature*, vol. 323, no. 6088, pp. 533–536, Oct. 1986.
[32] J. Duchi, E. Hazan, and Y. Singer, "Adaptive subgradient methods for online learning and stochastic optimization," *J. Mach. Learn. Res.*, vol. 12, pp. 2121–2159, Feb. 2011.
[33] G. Hinton, N. Srivastava, and K. Swersky, "RMSProp: Divide the gradient by a running average of its recent magnitude," *COURSERA, Neural Netw. Mach. Learn.*, vol. 4, no. 2, pp. 26–31, 2012. [Online]. Available: https://www.coursera.org/learn/neuralnetworks/lecture/YQHki/rmsprop-divide-the-gradient-by-a-runningaverage-of-its-recent-magnitude
[34] D. P. Kingma and J. Ba, "Adam: A method for stochastic optimization," 2014, *arXiv:1412.6980*. [Online]. Available: http://arxiv.org/abs/1412.6980
[35] S. Makonin and F. Popowich, "Nonintrusive load monitoring (NILM) performance evaluation," *Energy Efficiency*, vol. 8, no. 4, pp. 809–814, Jul. 2015.

JIN-WOOK LEE received the B.E. degree in energy and IT and the M.S. degree in electrical engineering from Gachon University, South Korea, in 2017 and 2019, respectively, where he is currently pursuing the Ph.D. degree in electrical engineering with the Smart Green Home Research Center. His research interests include grid impact in distribution systems, optimization, dc grid, AI, and smart grid.

KEON-JUN PARK (Member, IEEE) received the B.S. degree in electrical and electronics engineering from Wonkwang University, Iksan, South Korea, in 2003, and the M.S. degree in control and instrumentation engineering and the Ph.D. degree in electrical engineering from the University of Suwon, Suwon, South Korea, in 2005 and 2010, respectively. He is currently a Research Professor with the Smart Green Home Research Center, Gachon University, South Korea. His research interests include computational intelligence, intelligence modeling, and applications in smart grids.

JINTAE CHO received the B.S. and M.S. degrees in electrical engineering from Korea University, Seoul, South Korea, in 2006 and 2008, respectively, where he is currently pursuing the Ph.D. degree in dc distribution. He is a Senior Researcher with the Smart Power Distribution Laboratory, Korea Electric Power Corporation Research Institute (KEPRI), Daejeon, South Korea. His research interests include protection, monitoring, control of LVDC distribution systems, and automated distribution planning.

JU-YONG KIM received the M.S. and Ph.D. degrees from Kyungpook National University, Daegu, South Korea, in 1994 and 2007, respectively. He joined Korea Electric Power Corporation Research Institute (KEPRI), Daejeon, South Korea, as a Researcher, in 1994. He is currently the General Manager of the Distribution Planning Group, Smart Power Distribution Laboratory, KEPRI. His main research interests include dc distribution systems and dc microgrid.

SUNG-YONG SON (Member, IEEE) received the B.S. and M.S. degrees from the Korea Advanced Institute of Science and Technology (KAIST), South Korea, in 1990 and 1992, respectively, and the Ph.D. degree in mechanical engineering from the University of Michigan at Ann Arbor, Ann Arbor, in 2000. From 2000 to 2005, he worked at 4DHomeNet and iCross Technology. He was a Visiting Scholar with the Lawrence Berkeley National Laboratory (LBNL), in 2014. He is currently a Professor with the Department of Electrical Engineering, Gachon University, South Korea. His main research interests include smart grids, smart homes, and smart cities.